

Modeling and Simulation of the Sliding Motion of a 3-D Soft Fingertip with Friction, Focusing on Stick-Slip Transition

*VAN ANH HO (立命館大学), 平井 慎一 (立命館大学.)

Abstract—We have proposed a dynamic model to investigate the sliding motion of a 3-dimensional soft fingertip on a plane with friction. The fingertip is comprised virtually of a finite number of elastic compressible and bendable cantilevers whose free ends act as infinitesimal contact points. The contact surface is afterward is meshed based on coordinates of contact points. By introducing Coulomb's law and contact compliance into each contact point, we are able to assess the frictional characteristic during sliding motions of the fingertip, especially stick-slip motions. We also present experimental results to validate this model.

Key Words: Sliding soft fingertip, friction, FEA method, discrete method.

1. Introduction

Dexterous Manipulation is an area of robotics in which multiple manipulators, or fingers, cooperate in grasping and manipulating an object [1]. Much recent robotic research has focused on the dexterous manipulation of objects using soft fingered robotic hands, especially anthropomorphic ones. This type of research can be categorized into two main groups. The first consists of studies focusing on analyzing contact mechanics between various soft fingers and objects [2]. In the second, tactile sensing systems imitating those of humans, along with many types of sensors, have been developed to simulate human abilities in object grasping and dexterous handling [3]. Whereas the former studies consisted primarily of analysis of stable grasping or object postures controlled by utilizing soft fingertips' compliance during a pushing or rolling motion on the surface of objects; the latter studies concentrated on the tactile texture perceptions of sensory fingertips, to increase efficiency during object manipulation processes. Among various movements of fingertips during handling, slide/slip often occurs during any contact, and is considered important in dexterous manipulation [4]. For example, to assess the texture of an object's surface, the fingertip needs to slide slightly on the surface to extract information about its roughness or friction. The trend of sliding motion of the object between fingertips during grasping, or the incipient slip, is recognized as a crucial factor in stable object manipulation. However, while the latter studies have addressed all types of motion of the fingertips, such as pressing, rolling, and rubbing; the former studies have focused primarily on pure pushing and rolling movements, while ignoring slip or slide. The difficulties in modeling the sliding motion of fingertips comes from the compliance of fingertips, their partial movements on contact surfaces, and friction force/moment. Kao and Cutkosky in [5] have proposed a method that combines compliance and friction on a limited surface to compute the relative sliding motion between a grasped object and soft fingers. That article showed concrete results in modeling contact, and in approximate gross-motion planning. Fearing [6] introduced an algorithm for automatic stable grasping of polygonal objects with two fingers and point contact with friction. Nevertheless, most researches only deal with quasi-static analysis, gross sliding; not yet much consideration on stick-slip phases (how and when it happens), or partial slip on the contact surface of soft fingertip. In the other trend, FEA (Finite Element Analysis) model of contacting soft fingertip was also conducted. This method is time-consuming, and usually solved in static field.

We have attempted to determine the frictional characteristics of a 3-dimensional soft fingertip during unilateral sliding motion relative to an object dynamically. In doing so, we have proposed a method to model vertical and horizontal deformations of the soft fingertip during sliding. Moreover, we have modeled the contact by employing FEA method, in companion of Coulomb's frictional law. This permits to reduce remarkably calculation time, while still assure the dynamic behavior of the system during stick-slip transition.

2. Proposed Modeling of a Hemispherical Soft Fingertip

Previous research ([2]) proposed that a soft fingertip model comprised of an infinite number of vertical elastic virtual springs could be used to investigate the deformation of the fingertip during pushing or rolling motion on an object. This model, however, was not sufficient to demonstrate sliding motion with the appearance of frictional force. In the other way, issues of modeling a 3-D (dimension) soft fingertip using FEA method were also addressed by employing potential of commercial FEA softwares ([7]). Most of work only deal with static analysis; moreover, it takes a remarkable amount of time to simulate 3-D FEA model. As a result, it is not possible to use these models in applications require realtime calculation.

We are attempting to combine two methods using both discrete and FEA methods to model a 3-D soft fingertip, with the appearance of friction in sliding motions, especially stick-slip transition. By doing so, the consuming time will be reduced remarkably, while assuring the correctness of the model. Assuming that a hemispherical soft fingertip with radius R is pushed vertically with contact depth d_n by normal force F_n on a rigid flat plane, and slid horizontally with external force F_t (Fig. 1(a)). This forms a circular contact surface between the fingertip and the plane with radius a , which is calculated as:

$$a = \sqrt{R^2 - (R - d_n)^2}. \quad (1)$$

Firstly, we mesh this 2-D contact surface using the Voight model to describe the elastic and viscous properties of the contact surface ([8]) on the O_{XY} coordinates. Each element is a triangle T_p with three nodes referred as P_i , P_j , and P_k in a counterclockwise direction (Fig. 1(b)). Because the fingertip can slide in any direction, the mesh of the contact surface must be symmetrical to the central point of the contact surface. Fig. 1(b) illustrates a possible mesh of the contact surface. Secondly, at position of each node on the O_{XY} coordinate, one corresponding elas-

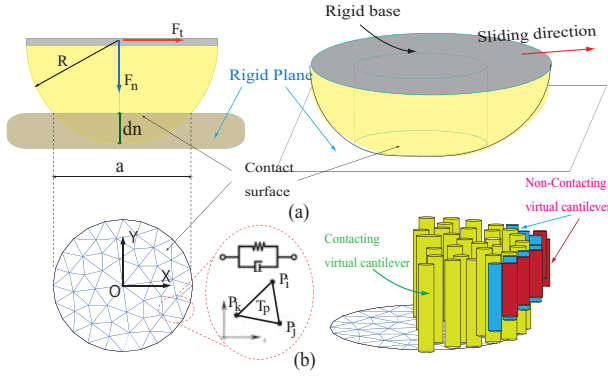


Fig.1 Model of a sliding soft fingertip with virtual cantilevers and meshed contact surface.

tic cantilever with cross-sectional radius r^i , and length l^i is put along Z-axis. By specifying proper values of (r^i , l^i) based on geometric distribution of contact nodes, we can fill the volume of the soft fingertip by cantilevers. These cantilevers are fixed on the equatorial surface of the fingertip, with their free ends on the contact surface. For the sake of simplicity, we made three assumptions:

1. When a cantilever is bent, its deformation is significant only at the free end.
2. Interactions between continuous cantilevers only occur between their free ends on the contact surface.
3. Only cantilevers whose free ends are acting on the contact surface are considered (dark green colored cantilevers in Fig. 1(b)). Cantilevers outside the contact surface are deemed irrelevant to the sliding motion of the fingertip (blue and red colored cantilevers in Fig. 1(b)).

As a result, when the fingertip is pushed and slid, its deformation will be represented by deformations of all the cantilevers. Moreover, external forces acting on each node on the contact surface can be assessed by calculating compress and bending forces of the corresponding cantilever. Especially, Coulomb friction model can be introduced into each node, which was usually neglected in the previous researches. Consequently, by combine both discrete and FEA methods into modeling the soft fingertip, it is expected to perceive dynamic behavior of the fingertip during sliding motion, especially stick-slip states.

3. Mathematical Approaches

3.1 For Cantilevers

Let us analysis one arbitrary cantilever, say i -th cantilever, which has coordinates in O_{XY} as (x_i, y_i) , Young's modulus E , natural length l_o^i , natural cross-sectional radius r_o^i . After being pushed with contact depth d_n^i , normal force f_n^i acting on the free end of this cantilever is computed as:

$$f_n^i = k^i d_n^i = E \frac{\pi r_o^{i2}}{l_o^i} \left\{ \sqrt{r^2 - (x_i^2 + y_i^2)} - (r - d_n) \right\}. \quad (2)$$

As a result, sum of normal forces acting on all cantilevers must equal to F_n , as:

$$F_n = \sum f_n^i. \quad (3)$$

When the external tangential force F_t starts to activate, the fingertip has not been slid yet. The contact surface still sticks to the

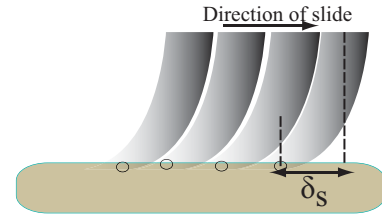


Fig.2 Bending strain during stick phase.

plane, causing the fingertip to deform. At this time, all contacting cantilevers are bent at the free ends with the same bending strain δ_s , as illustrated in Fig. 2. This bending strain is calculated as originated in [9]:

$$\delta_s = \frac{3\mu F_n}{16r} \frac{2-\nu}{G} \{1 - (1-\Phi)^{2/3}\}, \quad (4)$$

where $\Phi = F_t/\mu F_n$ is tangential force coefficient, μ is the friction coefficient of the contact area, and $G = E/2(1+\nu)$ with ν being Poisson ratio. By assessing the bending strain in eq. (4), bending force f_b^i acting on the free end of the cantilever is computed in the following equation:

$$f_b^i = b^i \delta_s = \frac{3EI}{(l^i)^3} \delta_s = \frac{3E\pi(r^i)^4}{(l^i)^3} \delta_s. \quad (5)$$

3.2 For 2-D FEA Contact Surface

There are many ways to solve FEA simulations of sliding contact using commercial softwares such as ANSYSTM, or MARCTM. However, they cannot extract the exact behavior of friction force, or micro slips during stick-slip transition. Therefore, we proposed a method to calculate dynamically the output of friction force, as well as micro sticks/slips on the contact surface during stick-slip transition. Let us define λ^{ela} , and μ^{ela} as elastic Lamé constants; λ^{vis} , and μ^{vis} as viscous Lamé constants. Connection matrices can be described as \mathbf{J}_λ , and \mathbf{J}_μ which can be obtained by synthesizing partial connection matrices set of triangles $\{T_p\}$. Detailed derivations of those matrices can be refereed in [10]. By using connection matrices, we can describe a geometric relationship between whole nodal points. Vectors of displacements, and velocities of N nodes on the contact surface are defined as \mathbf{u}_N , and \mathbf{v}_N , respectively. Let \mathbf{F}_{ve} be a visco-elastic force vector on contact nodes, then it can be calculated as:

$$\mathbf{F}_{ve} = (\lambda^{ela} \mathbf{J}_\lambda + \mu^{ela} \mathbf{J}_\mu) \mathbf{u}_N + (\lambda^{vis} \mathbf{J}_\lambda + \mu^{vis} \mathbf{J}_\mu) \mathbf{v}_N, \quad (6)$$

or:

$$\mathbf{F}_{ve} = \mathbf{K}_{ela} \mathbf{u}_N + \mathbf{K}_{vis} \dot{\mathbf{u}}_N. \quad (7)$$

For each node, beside visco-elastic force \mathbf{f}_{ve}^i calculated implicitly by eq. (7), there exist friction force $\mathbf{f}_{f,r}^i$, normal force \mathbf{f}_n^i , and bending force \mathbf{f}_b^i . To be capable to assess stick/slip motion of each contact node, slip condition is proposed based on Coulomb condition, and CSM (Constraint Stabilization Method). This method, when applied for a node, assures the fixture of that node. Let $\mathbf{A}_{2,2}^i$ be a matrix to describe the constraint of i -th node. If $\mathbf{A} = \mathbf{0}_{2,2} = \mathbf{A}_0^i$ then this node is unconstrained; while if

$\mathbf{A} = \mathbf{I}_{2,2} = \mathbf{A}_1^i$ then this node is fixed. As a result, stick/slip condition of a contacting node is described as follows:

$$\mathbf{f}_{fr}^i = \begin{cases} \mathbf{f}_{ve}^i + \mathbf{f}_b^i & \text{if } \mathbf{f}_{ve}^i + \mathbf{f}_b^i < \mu \mathbf{f}_n^i \Rightarrow \text{Stick} \Rightarrow \mathbf{A}^i = \mathbf{A}_1^i \\ \mu \mathbf{f}_n^i & \text{if } \mathbf{f}_{ve}^i + \mathbf{f}_b^i \geq \mu \mathbf{f}_n^i \Rightarrow \text{Slip} \Rightarrow \mathbf{A}^i = \mathbf{A}_0^i. \end{cases} \quad (8)$$

Constraint matrix \mathbf{A} of all nodes will be synthesized from partial constraint matrices as:

$$\mathbf{A}^T = \begin{pmatrix} \mathbf{A}^0 & \mathbf{O} & \dots & \mathbf{O} \\ \mathbf{O} & \mathbf{A}^1 & \dots & \mathbf{O} \\ \vdots & \vdots & \ddots & \vdots \\ \mathbf{O} & \mathbf{O} & \dots & \mathbf{A}^N \end{pmatrix}_{2N,2N}. \quad (9)$$

As a result, the geometric constraint is described in the following equation:

$$\mathbf{R} = \mathbf{A}^T \mathbf{u}_N = \mathbf{0}. \quad (10)$$

We apply the CSM to incorporate this constraint into dynamic equations. Let us define a critical damping of the constraint:

$$\ddot{\mathbf{R}} + 2\omega \dot{\mathbf{R}} + \omega^2 \mathbf{R} = \mathbf{0}, \quad (11)$$

where ω denotes a predetermined angular frequency. This equation turns into the following differential equation:

$$\mathbf{A}^T \ddot{\mathbf{u}}_N + \mathbf{A}^T (2\omega \dot{\mathbf{u}}_N + \omega^2 \mathbf{u}_N) = \mathbf{0}. \quad (12)$$

Consequently, Lagrangian under geometric constraint \mathbf{R} is formulated as:

$$\mathbf{L} = \mathbf{T} - \mathbf{U} + \mathbf{W} + \lambda^T \mathbf{A}^T \mathbf{u}_N, \quad (13)$$

or:

$$\mathbf{L} = \frac{1}{2} \dot{\mathbf{u}}_N^T \mathbf{M} \dot{\mathbf{u}}_N - \frac{1}{2} \mathbf{u}_N^T \mathbf{K}_{ela} \mathbf{u}_N - \frac{1}{2} \dot{\mathbf{u}}_N^T \mathbf{K}_{vis} \dot{\mathbf{u}}_N + \mathbf{f}^T \mathbf{u}_N + \lambda^T \mathbf{A}^T \mathbf{u}_N, \quad (14)$$

with \mathbf{M} being the inertia matrix of the 2-D FEA contact surface, $\mathbf{f} = \mathbf{f}_{fr} + \mathbf{f}_b$ being external force vector on the contact surface, and λ being a set of Lagrange multipliers. Therefore, a set of motion equations of all nodal points is formulated as:

$$-\mathbf{M} \ddot{\mathbf{u}}_N - \mathbf{K}_{ela} \mathbf{u}_N - \mathbf{K}_{vis} \dot{\mathbf{u}}_N + \mathbf{f} + \mathbf{A} \lambda = \mathbf{0}. \quad (15)$$

Recalling the eq. (12), and introducing the relation $\mathbf{v}_N = \dot{\mathbf{u}}_N$, equation motions of all nodes can be described as follows:

$$\begin{cases} \mathbf{v}_N = \dot{\mathbf{u}}_N \\ \mathbf{M} \dot{\mathbf{v}}_N - \mathbf{A}^T \lambda = -\mathbf{K}_{ela} \mathbf{u}_N - \mathbf{K}_{vis} \mathbf{v}_N + \mathbf{f} \\ -\mathbf{A}^T \dot{\mathbf{v}}_N = \mathbf{A}^T (2\omega \mathbf{v}_N + \omega^2 \mathbf{u}_N) \end{cases} \quad (16)$$

This equation is linear and be solved since the matrix is regular, resulting $\dot{\mathbf{u}}_N$, and $\dot{\mathbf{v}}_N$. Moreover, we also can perceive the friction force acting on each node during its stick/slip, as well as total friction force on the contact surface. As a result, a dynamic look at the contact surface during stick-to-slip phase is made clear, by solving equation (16).

4. Simulation

All code of the program were implemented in C++ programming environment to optimize the calculation time. To solve the eq. (16), we employed a six order Runge-Kutta method with a sampling time of 1.0×10^{-6} s. In this simulation, the soft fingertip has diameter of 10.0 mm, which is similar to adult thumb's fingertip; and it is pushed with contact depth $d_n = 2.0$ mm, and slid with constant velocity $v = 5.0$ mm/s. The Young's modulus is $E = 0.232$ MPa, and Poisson ratio is $\nu = 0.48$. Simulation is focused on stick-to-slip transition, which means the transient phase before the stable slide of the fingertip. The friction coefficient is predetermined as $\mu = 0.9$, the number of contact nodes is $N = 57$.

In Fig. 3, there is the plot of friction force acting on the contact surface during stick-to-slip phase. It is calculated by sum up all friction forces acting on nodes of the contact surface. It is easy to realize to different stages of friction force during this phase. In the stick stage, the friction force keeps increasing, while it is unchanged in the slide stage. There is no sudden change between two stages; it happens smoothly. Moreover, by illustrating partial trajectories of contact nodes during the stick-to-slip transition in Fig. 4, we can perceive a close look at micro changes of strain on the contact surface. That is, peripheral area of the contact surface slips first (Fig. 4(a)); the slipping area is extending to the central of the contact surface in Fig. 4(b) to (c); and finally is the moment right before the entire contact surface slips (Fig. 4(d)). This is well known as incipient slip of a hemispherical soft fingertip, and has been mentioned experimentally in many researches ([1], [3]). The simulation time is about 4 minutes for a PC running WindowXP, Intel Processor 1.8 GHz. It is much smaller than 3-D simulations of static sliding motion using commercial softwares which take about some hours. By using GNU in the future, this simulation can be implemented in realtime.

In summary, by simulating the proposed model of a sliding hemispherical soft fingertip in the stick-to-slip transition, we not only assess the response of the friction force, but also partial slips on the contact surface during this phase. This is considered a contribution in explaining theoretically an issue which was proposed experimentally in the research beforehand.

5. Experimental Validation

To verify the simulated model, we conducted an experiment in which one polyurethane rubber soft fingertip is slid on a rigid surface by a 2-DOF stage. A 3-DOF loadcell is attached upon the fingertip to measure external forces acting on it. Moreover,

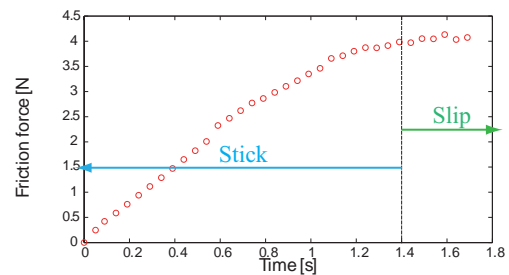


Fig.3 Friction force during stick-to-slip transition.

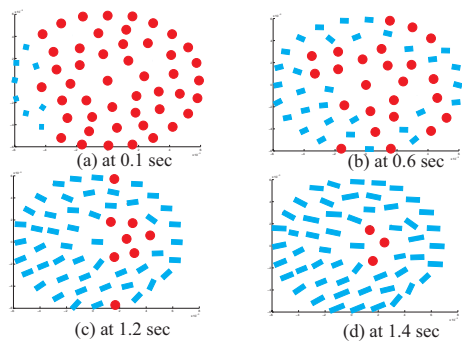


Fig.4 Simulation's micro displacements on the contact surface during stick-to-slip transition. Red dots illustrate stick contact nodes; blue bars show trajectories of slipped contact nodes.

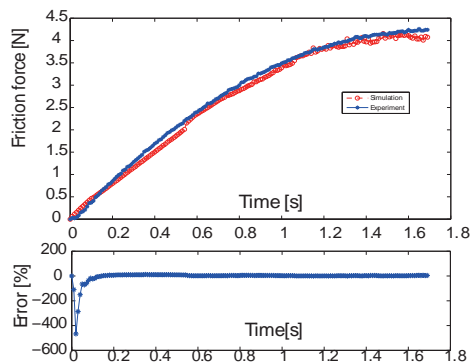


Fig.5 Comparison between simulation and experiment's friction force at $v = 5.0$ mm/s.

on the outer surface of the fingertip, there are marking dots used to emulate contacting nodes. A high speed camera was employed to track movements of these dots. In Fig. 5(a) is comparison between simulated and experimented friction forces during stick-to-slip transition with $v = 5.0$ mm/s. We can observe the fine agreement between two results. The relative error is large at the very beginning moment of the slide, but quickly goes to zero, as illustrated in Fig. 5(b). The similarity is also assessed when the velocity is decreased to $v = 2.0$ mm/s as plotted in Fig. 7. In Fig. 6, there are processed images of contact surface with trajectories of marking dots during stick-to-slip transition. Similar conclusion can be made by observing these images compared to that of simulation results.

6. Conclusion

We have investigated stick-slip transition of a sliding hemispherical soft fingertip with friction. By employing model of the soft fingertip with finite number of elastic cantilevers, and FEA contact surface, our model is able to extract dynamically in detail micro slips on the contact surface, including orders of their movements. Moreover, by using this model, simulation time has been reduced significantly to some minutes in a common PC desktop. In the future, we will implement the program using GNU computer and parallel computations toward the realtime modeling and simulation. By doing so, it will be capable to use the model in compensate friction in controlling sliding motions of robotic soft fingertip to enhance the quality of control.

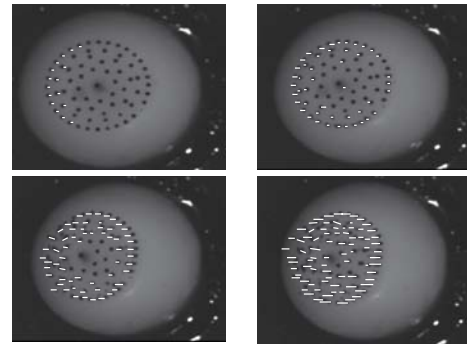


Fig.6 Experiment's micro displacements on the contact surface during stick-to-slip transition. White bars show trajectories of slipped contact nodes.

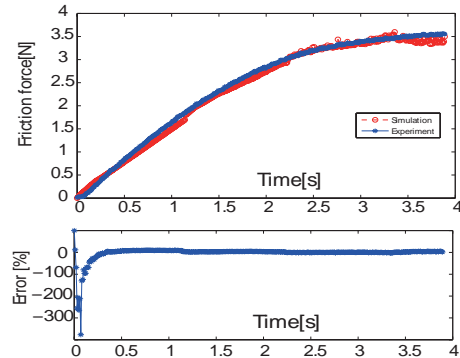


Fig.7 Comparison between simulation and experiment's friction force at $v = 2.0$ mm/s.

Reference

- [1] A. M. Okamura, N. Smaby, and M. R. Cutkosky *An Overview of Dexterous Manipulation*, IEEE Int. Conf. Robot. Autom. Symposium, May 2000.
- [2] T. Inoue, S. Hirai, *Elastic Model of Deformable Fingertip for Soft-Fingered Manipulation*, IEEE Transaction on Robotics, vol. 22, no. 6, December 2006.
- [3] L. Beccai, S. Roccella, L. Ascari, P. Vandastrì, A. Sieber, M. C. Carrozza, P. Dario *Development and Experimental Analysis of a Soft Compliant Tactile Microsensor for Anthropomorphic Artificial Hand*, IEEE Transaction on Mechatronics, vol. 13, no. 13, April 2008.
- [4] A. M. Okamura, Micheal L. Turner, and Mark R. Cutkosky *Haptic Exploration of Objects with Rolling and Sliding*, IEEE Int. Conf. Robot. Autom., vol. 3, pp. 2485-2490, May 1997.
- [5] I. Kao, M. R. Cutkosky, *Quasistatic Manipulation with Compliance and Sliding*, The Int. Jour. of Robotic Research, Vol. 11, No. 1, pp. 20-40, Feb. 1992.
- [6] R. S. Fearing, *Implementing a force strategy for object reorientation*, IEEE Int. Conf. on Robotics and Autom., vol. 3, pp. 96-102, April 1986.
- [7] T. Maeno, S. Hiromitsu, and T. Kawai, *Control of Grasping Force by Detecting Stick/Slip Distribution at the Curved Surface of an Elastic Finger*, IEEE Int. Conf. on Robotics and Autom., pp. 3895-3900, April 2000.
- [8] J. L. Johnson, *Contact Mechanics*, Cambridge, U.K., Cambridge Univ. Press, 1984
- [9] R. D. Mindlin, *Compliance of elastic bodies in contact*, Trans. ASME, J. Appl. Mech., vol. 16, pp. 259-268, 1949.
- [10] K. Namima, Z. K. Wang, and S. Hirai, *Simulation of Soft Fingertip Deformation under Contact and Rolling Constraints using FEM and CSM*, IEEE Int. Conf. on Robotics and and Biomimetics, pp. 1585-1590, Dec. 2010.